Characterizing Thermal Mixing Dynamic Nuclear Polarization via Cross-Talk between Spin Reservoirs

David Guarin, Sina Marhabaie, Alberto Rosso, Daniel Abergel, Geoffrey Bodenhausen, Konstantin L. Ivanov, Dennis Kurzbach

Characterizing Thermal Mixing Dynamic Nuclear Polarization via Cross-Talk between Spin Reservoirs

David Guarin,[†,‡] Sina Marhabaie,[†,‡] Alberto Rosso,[†,§] Daniel Abergel,[†,‡] Geoffrey Bodenhausen,[†,‡] Konstantin L. Ivanov,[*,∥,⊥] and Dennis Kurzbach[*,†,‡]

[†]Département de Chimie, Ecole Normale Supérieure, PSL Research University, UPMC Univ Paris 06, CNRS, Laboratoire des Biomolécules (LBM), 24 rue Lhomond, 75005 Paris, France

[‡]Sorbonne Universités, UPMC Univ Paris 06, Ecole Normale Supérieure, CNRS, Laboratoire des Biomolécules (LBM), 75005 Paris, France

[§]Laboratoire Physique Théorique et Modèles Statistiques (LPTMS), Université Paris-Sud, Université Paris-Saclay, CNRS, 91405 Orsay, France

[∥]International Tomography Center SB RAS, Institutskaya 3a, Novosibirsk 630090, Russia

[⊥]Novosibirsk State University, Pirogova 2, Novosibirsk 630090, Russia

ABSTRACT: Dynamic nuclear polarization (DNP) embraces a family of methods to increase signal intensities in nuclear magnetic resonance (NMR) spectroscopy. Despite extensive theoretical work that allows one to distinguish at least five distinct mechanisms, it remains challenging to determine the relative weights of the processes that are responsible for DNP in state-of-the-art experiments operating with stable organic radicals like nitroxides at high magnetic fields and low temperatures. Specifically, determining experimental conditions where DNP involves thermal mixing, which denotes a spontaneous heat exchange between different spin reservoirs, remains challenging. We propose an experimental approach to ascertain the prevalence of the thermal mixing regime by monitoring characteristic signature properties of the time evolution of the hyperpolarization. We find that thermal mixing is the dominant DNP mechanism at high nitroxide radical concentrations, while a mixture of different mechanisms prevails at lower concentrations.

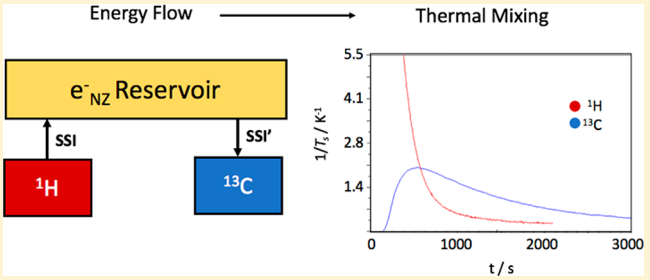

Dynamic nuclear polarization (DNP) is a powerful method for enhancing the polarization of nuclear spins with the aim of boosting weak nuclear magnetic resonance (NMR) signals. In recent years, DNP has experienced a remarkable "renaissance" due to novel methodological developments, in particular for solid-state DNP (MAS-DNP)[1−4] and dissolution DNP (D-DNP),[5−10] which enables many new applications in practically all fields of NMR[10,11] and MRI[5,7] ranging from in-cell metabolomics to cancer monitoring in humans. At the heart of DNP lies the transfer of electron spin polarization to nuclear spins upon pumping electron paramagnetic resonance (EPR) transitions of stable mono- or biradicals. To widen the range of applications of DNP and to optimize the enhancements, a thorough understanding of the underlying mechanisms is a prerequisite. At this time, five distinct DNP mechanisms are known to play a role in solids:[12−14] the solid effect (SE), the differential solid effect (DSE), the cross-effect (CE), thermal mixing (TM) and the Overhauser effect (OE). While the latter exploits dissipative cross-relaxation, the former four mechanisms make use of coherent polarization transfer. The SE is due to pumping "forbidden" combinations of EPR and NMR transitions; since it involves an isolated electron spin and an isolated nuclear spin, this mechanism is most efficient when using dilute monoradicals. A more efficient DNP mechanism that dominates for dilute biradicals or concentrated monoradicals is provided by the CE, which requires a pair of electron spins so that "triple spin flips" (of two electron spins, SS', and one nuclear spin) can occur (denoted $SS'I$ for $I = {}^{1}\mathrm{H}$, or $SS'I'$ for other nuclei I' such as $^{2}\mathrm{H}$, $^{13}\mathrm{C}$, $^{31}\mathrm{P}$, etc.) Finally, concentrated monoradicals with strong intermolecular interactions can lead to TM, a mechanism for which thermodynamic concepts can be used[15−17] to describe polarization transfer in terms of heat exchange between different reservoirs. TM is effective only when the EPR spectral width $\Delta\nu_e$, given either by homogeneous line broadening or electronic spectral diffusion (eSD), exceeds the nuclear Zeeman interaction frequency ν_I.[18,19]

Various definitions for TM have been given.[14−17] Here we consider that TM entails three important properties. (1) Electron spins, even under microwave irradiation, display a behavior that can be described using thermodynamic concepts. Namely, their description involves two heat reservoirs: a

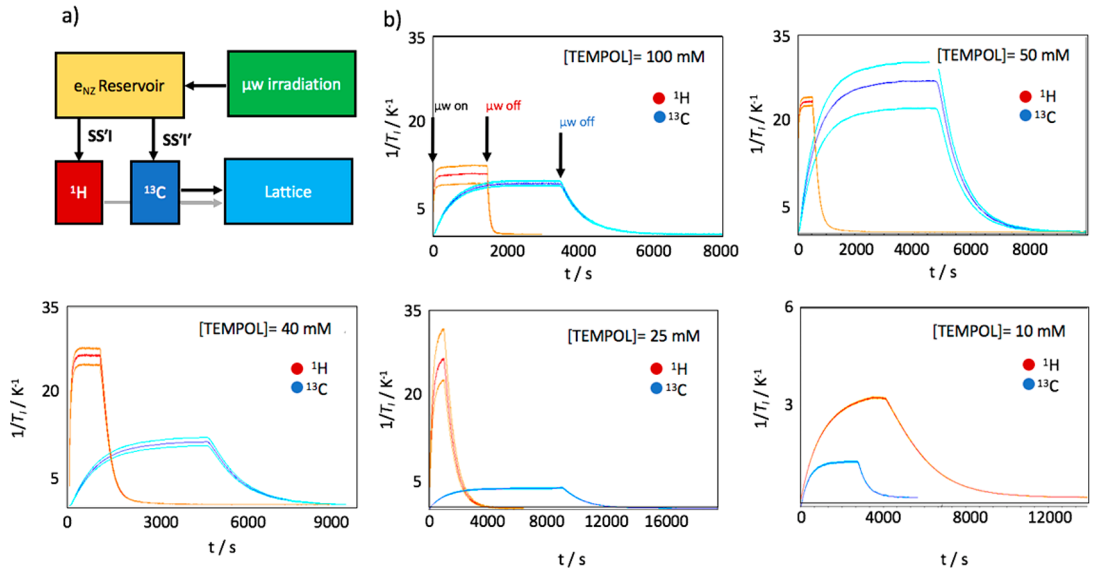

Figure 1. (a) Energy reservoirs involved in experiment **A** that monitors the buildup of the polarizations $P(I = {}^1\mathrm{H})$ and $P(I' = {}^{13}\mathrm{C})$ after switching on the saturation of the EPR spectrum by microwaves (μw), and their decay after interruption of the μw irradiation. The μw irradiation cools down the non-Zeeman dipolar electron reservoir e_{NZ}; as a result, the ^{1}H and ^{13}C spins are polarized simultaneously via heat exchange between the reservoirs. Nuclear relaxation proceeds via dissipation of energy to the lattice. (b) DNP build-up curves and decay of polarizations after switching off the μw-field (at the delays indicated exemplarily for ^{1}H and ^{13}C in the panel of 100 mM TEMPOL) for a sample containing $I = {}^1\mathrm{H}$ and $I' = {}^{13}\mathrm{C}$ nuclei. The polarizations are expressed in terms of inverse spin temperatures, $1/T_I$. Traces shown in lighter color indicate the ranges of experimental errors.

Zeeman reservoir, introduced to describe energy variations on the order the electronic Zeeman interaction ν_e, and a non-Zeeman or dipolar reservoir, to describe exchange of energy on the order of the relevant width $\Delta\nu_e$ of the EPR spectrum. (2) Triple-spin flips $SS'I$ can establish a contact between the nuclear Zeeman and electron non-Zeeman reservoirs,[19] since they involve the transfer of energy of the order of the nuclear Zeeman energy ν_I between nuclear and electron spins. (3) The rates of triple-spin flips are fast compared to the rates of other phenomena such as electron or nuclear relaxation rates.

Only if these properties are fulfilled can DNP proceed predominantly via TM. In this case, the hyperpolarization process displays two characteristic features:

(i) the spin temperatures T_I of all nuclear spin species converge to a single common value for long times $t \to \infty$ in the presence and absence of microwave irradiation. As a result, all nuclei I for which $\nu_I < \Delta\nu_e$ are "cooled down" in the same way at all microwave frequencies, in contrast to SE and CE where the microwave frequency for most efficient DNP depends on the nuclear gyromagnetic ratio, γ_I.

(ii) A second important consequence of TM is that, if different types of nuclei are present in the sample, heat can flow spontaneously from one nuclear reservoir to another via the non-Zeeman electron reservoir. In other words, if TM is predominant, polarization transfers between different nuclear species are expected to follow the simple laws of heat propagation.

In practice, DNP often results not from a single dominant mechanism, but from a combination of different processes such that it may be difficult to separate contributions of different mechanisms.[16,20–22] A common strategy for the analysis of DNP processes is to simulate experimental results and to assess the underlying mechanism by comparing simulations and experiments. However, this approach is notoriously difficult even for discriminating SE and CE contributions.[19] When TM comes into play, the superposition of various mechanisms becomes even more difficult to unravel.

Therefore, it is currently not clear what DNP mechanisms are active for the frequently used nitroxide-radicals,[23] in particular at high magnetic fields $B_0 > 6$ T at $T < 1.2$ K for D-DNP or 20 T at 100 K for MAS-DNP.

Here we propose an experimental approach that allows one to determine whether TM is the predominant mechanism in state-of-the-art systems employing nitroxide radicals, based on probing the above-mentioned characteristic features (i) and (ii).

To elucidate the active DNP mechanism and to quantify the flow of polarization between different heat reservoirs via triple spin flips, we performed DNP experiments on spin systems comprising protons $I = {}^1\mathrm{H}$ and other nuclei ($I' = {}^2\mathrm{H}$, ^{13}C and ^{31}P) in the presence of radicals at variable concentrations. The experiments were carried out in two different ways: (A) we monitored the build-up curves of the polarization $P(I)$ and $P(I')$ of two different nuclei I and I' in the presence of microwave saturation of the EPR spectrum, and subsequently measured their return to thermal equilibrium after interrupting the microwave irradiation; (B) we performed in a systematic way an experiment proposed by Goldman and coauthors for single crystals of LiF (where $I = {}^7\mathrm{Li}$ and $I' = {}^{19}\mathrm{F}$), and adapted it to the case of amorphous solids that are used in modern DNP applications.[18] In this experiment, we polarized two different nuclei (here $I = {}^1\mathrm{H}$ and $I' = {}^2\mathrm{H}$, ^{13}C or ^{31}P), stopped saturating the EPR transitions, then depolarized one of the nuclei by rf saturation, and observed the subsequent time-dependence of polarizations $P(I)$ and $P(I')$. This includes a possible spontaneous transfer of polarization between nuclear spin species via the dipolar electron reservoir, which is a clear indication of so-called triple spin flips ($SS'I$ and $SS'I'$ flips). These two experiments hence allowed us to monitor to determine whether TM was the dominant mechanism for DNP or not.

EXPERIMENTAL SECTION

Sample Preparation. Sample **1** consisted of glycerol-d_8, D_2O and H_2O (50:40:10% in volume). Sample **2** consisted of the same mixture, with additional 1.5 M pyruvate-1-^{13}C. Sample **3** consisted of glycerol, glycerol-d_8, D_2O, and H_2O (with ratios 25:25:25:25% in volume). Sample **4** comprised the same solvent mixture of sample **1**, but contained 0.5 M K_2HPO_4 in addition. We used the nitroxide TEMPOL as characterized by a broad inhomogeneous EPR line (ca. 0.5 GHz). The TEMPOL concentration was varied in the range of 10−100 mM.

DNP. Our DNP apparatus is described in detail in references.[24−26] All samples were immersed in liquid helium at 4.2 K in the cryostat at atmospheric pressure. An ELVA1 microwave source coupled to a Virginia Diodes (VDI) frequency doubler provided microwaves (μw) at a frequency $\nu_{\mu w}$ = 187.9 GHz for all experiments **A** and **B**. The μw-field was modulated over a range of 100 MHz using a sawtooth modulation function with a 1 kHz repetition rate. The microwave frequency profiles were obtained by stepping the central frequency over a range 187.8 < $\nu_{\mu w}$ < 188.4 GHz with a 20 MHz step size and the same modulation bandwidth.

We used two-channel NMR probes to detect the polarization of both protons and heteronuclei $I' = {}^2H$, ^{13}C or ^{31}P at B_0 = 6.7 T. Although TM-DNP leads to higher nuclear polarizations $P(I)$ at 1.2 K, the sample temperature was set to 4.2 K to speed up the polarization build-up and shorten nuclear spin relaxation times, so that the experiments could be run faster. Thus, the inverse sample temperature (and electron spin temperature before microwave saturation) at thermal equilibrium was $1/T_0$ = 0.25 K^{-1}.

In experiment **A**, the nuclei $I = {}^1H$ and $I' = {}^{13}C$ were polarized through continuous-wave (cw) μw irradiation to determine the steady-state polarization and the characteristic build-up times of the nuclei. After achieving the steady state, the μw irradiation was interrupted to determine $T_1(I)$ and $T_1(I')$ decay times. Experiment **B** consisted of polarizing ^1H nuclei to their steady state by cw μw irradiation prior to switching off the μw source. The ^{13}C nuclei were then selectively saturated and the time evolution of both ^1H and ^{13}C nuclei was subsequently monitored in the absence of μw-irradiation. Saturation was achieved by a series of NMR pulses.

In all experiments, 1° detection pulses were used for $I = {}^1H$ and 5° pulses for I' nuclei at intervals of 5 s to monitor the signal intensity as a function of time.

RESULTS AND DISCUSSION

To elucidate the limits of TM, we systematically varied the experimental conditions for experiments **A** and **B**, to probe the two characteristic signatures (i) and (ii) listed above.

(1) Reaching a Common Spin Temperature. Figure 1a displays schematically the flow of spin order in experiment **A**. Our μw polarizes the non-Zeeman dipolar electronic (e_{NZ}) energy levels by cooling down the corresponding heat reservoir. Consequently, triple spin flips tend to equalize the e_{NZ} spin temperature and the nuclear spin temperature of both ^1H ($SS'I$ flips) and ^{13}C ($SS'I'$ flips) heat reservoirs. After switching off the μw irradiation, both nuclear polarizations $P(^1H)$ and $P(^{13}C)$ decay and equilibrate at the lattice temperature. Typical DNP build-up curves of these nuclear spin polarization and subsequent decays, obtained for different concentrations of TEMPOL, are shown in Figure 1b (sample **2**).

At all radical concentrations, the nuclei $I = {}^1H$ and $I' = {}^{13}C$ have different DNP buildup times and different relaxation times. The polarizations are expressed in units of $1/T_I$, the inverse spin temperature of the corresponding nucleus. The relation between the nuclear spin polarization, $P(I)$, and the inverse spin temperature $\beta_I = 1/k_B T_I$, is

$$P(I) = \tanh\left[-\frac{\hbar\omega_I}{2k_B T_I}\right] = \tanh\left[-\frac{\beta_I \hbar\omega_I}{2}\right] \quad (1)$$

where ω_I is the nuclear Zeeman resonance frequency in the external field. It is readily seen in Figure 1b that at TEMPOL concentrations above 50 mM, both nuclei converge to a common spin temperature after the initial build-up. In particular, $1/k_B T_I(^{13}C)$ reaches a maximum when the TEMPOL concentration is 50 mM. Most importantly, at lower radical concentrations (10−40 mM), the ^{13}C spin temperature is considerably higher than the proton one, thus indicating that TM is not the dominant mechanism since condition (i) listed above is not fulfilled anymore.[12]

The fact that TM no longer dominates at low radical concentrations originates from reduced rates of electron−electron flip-flops as the distance between radical centers becomes larger. On the one hand, when electron spectral diffusion slows down due to decreasing flip-flop probabilities, the electron spins cannot be treated anymore using thermodynamic concepts. Indeed, in this limit, the microwave irradiation will only saturate a narrow band around $\nu_{\mu w}$ in the EPR spectrum (hole burning), leaving the remaining electron spins at thermal equilibrium with the lattice. On the other hand, the rate of triple-spin flips decreases dramatically and becomes lower than the relaxation rates of the different spin species, leading to breakdown of the thermodynamic description of DNP.

The breakdown of the pertinence of the spin temperature concept at low radical concentrations has been recently predicted by numerical simulations that show a behavior consistent with our observations on ^{13}C. The strength of the thermal contact between the e_{NZ} reservoir and the nuclear Zeeman reservoir decreases steadily when reducing the radical concentration, down to a point where the thermodynamic description of DNP breaks down and hyperpolarization becomes less effective.[27,28]

(2) Heat Transfer between the Nuclear Zeeman Reservoirs. We can evaluate the presence of triple-spin flips at different radical concentrations by experiment **B**, schematically depicted in Figure 2a. Triple spin flips offer a mechanism through which the transfer of polarization, i.e., of heat from one nuclear reservoir to another via the e_{NZ} reservoir, can take place. Hence, a spontaneous heat flow from a warmer to a colder spin reservoir attests for the presence $SS'I$ triple-spin flips. Through our experimental setup, we could observe the transfer of polarization from ^1H to ^{13}C, i.e., as the ^1H reservoir heats up, the ^{13}C reservoir cools down. When the rate of triple spin flips is high, the two nuclear and the e_{NZ} reservoirs reach a common spin temperature before they relax to the equilibrium temperature. This is exactly what is observed in Figure 2b between 40 and 100 mM, where the ^{13}C polarization of sample **2** reaches a maximum when the temperatures of the two nuclear reservoirs become equal (the time traces cross). As such a polarization transfer proceeds via the electronic non-Zeeman reservoir, it can be investigated experimentally by stepping away from ideal TM conditions, e.g., by using lower

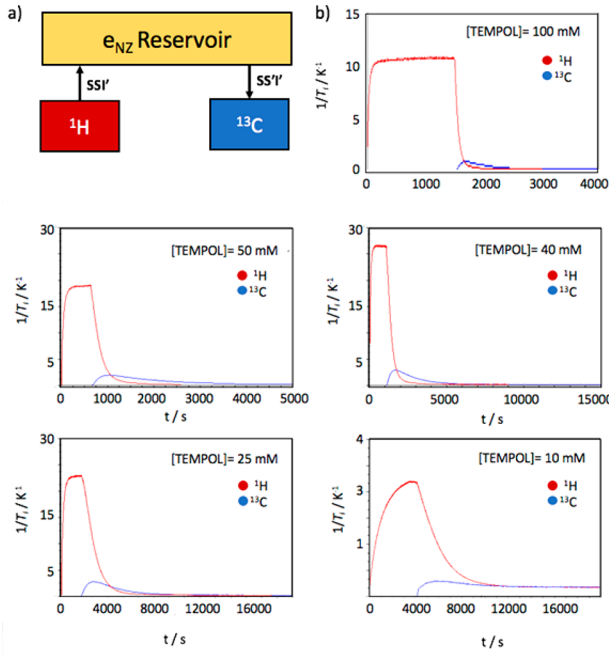

Figure 2. (a) Energy reservoirs involved in experiment **B** that monitors the transfer between the polarizations $P(I = {}^1\mathrm{H})$ and $P(I' = {}^{13}\mathrm{C})$ after the interruption of the μw irradiation and saturation of either I or I' nuclear reservoirs. Via triple spins flips, the polarization flows from ^{1}H to the non-Zeeman dipolar electron reservoir, and is then transferred to ^{13}C spins via $SS'I'$ triple spin flips. These processes are accompanied by relaxation to the lattice (omitted in the flow diagram). (b) Time evolution of the inverse nuclear spin temperature $1/T_I$. First, a polarization $P(I = {}^1\mathrm{H})$ is generated by DNP. Subsequently, after the μw irradiation is interrupted, the ^{13}C spins are saturated, and a spontaneous flow of polarization from ^{1}H to ^{13}C reservoirs is observed. Spontaneous transfer of heat from the ^{1}H to ^{13}C reservoir is indicative of triple spin flips $SS'I$ and $SS'I'$.

concentrations of radicals or by using radicals with narrow EPR lines.

To our surprise, the transfer of polarization between the two nuclear reservoirs is not entirely suppressed, even at a radical concentration as low as 10 mM. Thus, even though the signature features of a common spin temperature and an efficient heat transfer are not fulfilled, we observe triple spin flips, indicating a non-TM regime with a reduced rate of such transitions.

Through this, at radical concentrations of 25 mM and below we observe an "anomalous" heat transfer as the maximum inverse spin temperature $1/k_B T_I(C13)$ is reached at a time where $1/k_B T_I({}^1\mathrm{H})$ is still higher.

These data clearly confirm the presence of triple spin flips and transfer of polarization between the Zeeman reservoirs of the ^{1}H and ^{13}C nuclei and the non-Zeeman electronic reservoir, but point to the fact that the rates of triple spin flip transitions involving ^{13}C spins are comparable to or lower than their nuclear relaxation rates, impeding the prevalence of TM as dominant DNP mechanism.

In conclusion, at TEMPOL concentrations of 50 mM or above all characteristic features of TM, as defined above in points (i) and (ii), are observed, while at lower concentrations the nuclear reservoirs do not reach a common spin temperature; the heat transfer is inefficient despite the occurrence of triple spin flips.

The characteristic build-up times and steady-state spin temperatures at the end of the build-up (experiment **A**) as well as the transfer times (characteristic cooling times of the ^{13}C reservoir in experiment **B**) are summarized in Figure 3. Note that heat transfer becomes faster with increasing radical concentration (Figure 3c), thereby confirming the dependence of the triple spin flip rate on the TEMPOL concentration.

Changing Hyperpolarized Nuclei. To shed more light on the mechanistic details at intermediate TEMPOL concentrations, where features (i) (similar spin temperatures) and (ii) (characteristic heat transfer) of TM are not fulfilled, but triple spin flips are still observed via experiment **B**, we measured the dependence of the spin polarization $P(I')$ of the four nuclei $I' =$ ^{1}H, ^{13}C, ^{2}H and ^{31}P on the microwave irradiation frequency $\nu_{\mu w}$ at 25 mM TEMPOL. The profiles are shown in Figure 4. When TM is dominant, the widths of the μw-profiles would primarily depend the properties of the EPR spectrum of TEMPOL.[12,19] However, it is readily seen that the profiles for ^{1}H and ^{2}H are similar, while they differ significantly from those of ^{13}C and ^{31}P, which show slight differences between each other. In cases of CE or SE, one would expect a frequency difference of ν_I or $2\nu_I$, respectively, between the maxima and minima of the microwave profiles and thus a strong dependence on the nuclear gyromagnetic ratio.

Since none of these features is observed for any nuclei, we assume a mixture of different mechanisms for the low radical concentration regime. For ^{1}H and ^{2}H we observe profiles where the extrema are separated by ca. 440 MHz (more than the

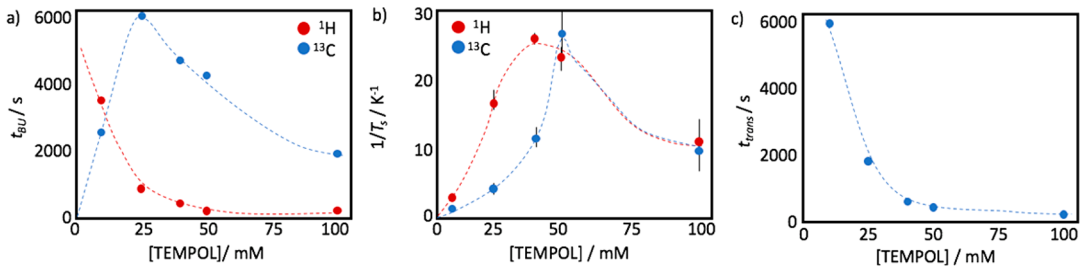

Figure 3. (a) Characteristic build-up times, t_{BU} for $P({}^1\mathrm{H})$ and $P({}^{13}\mathrm{C})$ polarizations at different TEMPOL concentrations, obtained by fitting experimental build-up curves to monoexponential functions. At low radical concentrations, the buildup of $P({}^{13}\mathrm{C})$ is faster than the buildup of $P({}^1\mathrm{H})$, indicating a change of the dominant DNP regime (see text for details). (b) Dependence of the inverse steady-state spin temperatures $1/T_I({}^1\mathrm{H})$ and $1/T_I({}^{13}\mathrm{C})$ as a function of the radical concentration. At a TEMPOL concentration of 50 mM, these inverse spin temperatures are similar within experimental error, indicating that TM is predominant, while below 40 mM this is no longer the case. (c) Characteristic polarization transfer times from $P({}^1\mathrm{H})$ to $P({}^{13}\mathrm{C})$ obtained by fitting the first part of the ^{13}C time dependence in experiment **B** to monoexponential build-up functions. The dashed lines are to guide the eye.

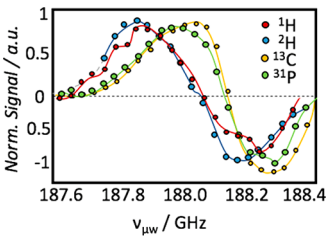

Figure 4. Dependence of nuclear signal intensities on the microwave frequency ("μw profiles") detected for ^{1}H (sample **1**), on ^{13}C (sample **2**), on ^{2}H (sample **3**) and on ^{31}P (sample **4**). In all cases, the frequency differences between the maxima and minima of the μw profiles do *not* correspond to multiples of ω_I, indicating significant contributions of TM; however, slight differences between the profiles indicate admixtures of SE and CE.

proton Larmor frequency, which is ν_I = 285.3 MHz at 6.7 T), and for ^{13}C and ^{31}P the extrema are separated by ca. 300 MHz. Vega, Han, and co-workers[13,14,16] have shown, based on simulations of experimental data under similar conditions, that at 25 mM TEMPOL for ^{1}H, a combination of CE and DSE can reproduce the experimental observations, in agreement with our observation that the ^{1}H and ^{13}C spin reservoirs do not reach a common spin temperature at this radical concentration. This indicates that the description of the DNP process as "pure" TM breaks down. We observe a similar behavior for ^{2}H, ^{13}C and ^{31}P. Note that the difference between the μw profiles characteristic for TM and CE is very subtle (the μw profiles for ^{1}H can be reproduced both with TM-based as well as CE-based models).[13,24]

Interestingly, we observe for all these nuclei triple spin flips via experiment **B** at 25 mM TEMPOL (see Figure 5).

For pairs of I = ^{1}H with I' = ^{13}C, ^{2}H or ^{31}P, one finds a spontaneous heat transfer via the e_{NZ} reservoir (see Figure 5a,b for the spin temperature as a function of time for I' = ^{2}H and ^{31}P). This clearly shows that the presence of triple spin flips is not a sufficient condition for TM, though a necessary one, if we assume TM as strictly defined by the signature features listed above.

Additionally, in experiment **B**, the heat transfer between ^{13}C and ^{1}H via the e_{NZ} reservoir with 50 mM TEMPOL works both ways (see Figure 5c), which confirms the consistency of our interpretation. In contrast, radicals with narrow EPR lines like 50 mM BDPA do not lead to any observable heat transfer in experiment **B**. This excludes direct cross-talk between the nuclear reservoirs (data not shown).

CONCLUSIONS

Combining experiments **A** and **B** yields a strategy for the determination of TM contributions to DNP, corresponding to the limiting case where the spin temperatures of all spin reservoirs tend to a common value T_I for $t \rightarrow \infty$ due to triple spin flips and the spontaneous heat transfer between different reservoirs. This strategy allows one to assess the presence of the TM regime, understood as a situation where a common nuclear spin temperature emerges from a spontaneous heat flow, through triple spin flip transitions. These two necessary conditions must both be fulfilled to establish TM, while one of them alone is insufficient. We want to stress that the sole occurrence of triple spin flips, or of spontaneous heat transfer, is not indicative of strict TM, if the spin temperatures of the different nuclei in the system do not converge. It can be clearly stated that TM is the dominant mechanism at high TEMPOL concentrations (≥50 mM) at 4.2 K and 6.7 T, i.e., for experimental conditions frequently used in modern DNP experiments, while for lower TEMPOL concentrations (≤40 mM) the spin temperatures of the different reservoirs can be different. The latter fact, in combination with the observation of spontaneous heat transfer, indicates the presence of $SS'I$ flips outside of the TM regime, which corresponds to a mixture of different mechanisms. At TEMPOL concentrations of 10 mM, where we observe only very weak heat transfer (experiment **B** indicates the breakdown of $SS'I$ transitions), the DSE is the most likely mechanism, as pointed out by Han and co-workers.[13]

From theoretical considerations, we expect the TM regime to establish at even lower radical concentrations if the sample temperature or the external magnetic field are decreased. Considering that processes, which involve a heat flow, need to compete with electronic T_1 relaxation, it appears intuitive that conditions that prolong relaxation favor thermal mixing.

From the experimental point of view, it is important to note that the lowest ^{13}C spin temperature can be reached at TEMPOL concentrations of 50 mM due to low ^{1}H spin temperatures and the dominance of TM. Yet, even lower ^{1}H temperatures can be reached at a lower TEMPOL concentration of 40 mM because favorable saturation factors.[29,30] This information is crucial for users who cannot rely on cross-polarization techniques.[26] In this situation TM-DNP can be a remedy, since it not only allows one to hyperpolarize protons, but various other nuclei by exploiting additional pathways for efficient polarization transfer.

AUTHOR INFORMATION

Corresponding Authors

*E-mail: kurzbach@ens.fr (D.K.).

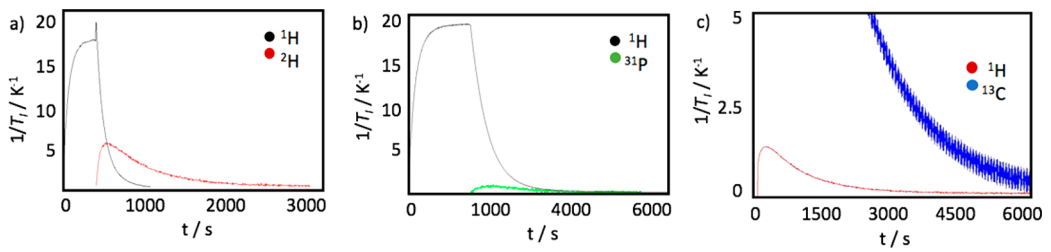

Figure 5. Experiments **B** for (a) sample **2** and (b) sample **4**. For both ^{2}H and ^{31}P a spontaneous polarization transfer from ^{1}H can be observed with 25 mM TEMPOL. (c) ^{13}C to ^{1}H polarization transfer in experiment **B** for sample 2 containing 50 mM TEMPOL after polarizing ^{13}C and saturating ^{1}H. Evidently, triple spin flips can transfer heat in both directions.

*E-mail: ivanov@tomo.nsc.ru (K.L.I.).
ORCID
Dennis Kurzbach: 0000-0001-6455-2136

Notes

The authors declare no competing financial interest.

■ ACKNOWLEDGMENTS

The authors thank Dr. Maurice Goldman for helpful discussions and Bruker BioSpin for providing a prototype of the DNP equipment. This work was supported by the French CNRS and the European Research Council contract "dilute para-water". K.L.I. acknowledges ENS (Paris) for a guest professorship and the Russian Foundation for Basic Research (Grant No. 17-03-00932). A.R. acknowledges ANR-16-CE30-0023-01 (THERMOLOC).

■ REFERENCES

(1) Valla, M.; Rossini, A. J.; Caillot, M.; Chizallet, C.; Raybaud, P.; Digne, M.; Chaumonnot, A.; Lesage, A.; Emsley, L.; van Bokhoven, J. A.; Coperet, C. Atomic Description of the Interface between Silica and Alumina in Aluminosilicates through Dynamic Nuclear Polarization Surface-Enhanced NMR Spectroscopy and First-Principles Calculations. *J. Am. Chem. Soc.* **2015**, *137*, 10710−10719.

(2) Lesage, A.; Lelli, M.; Gajan, D.; Caporini, M. A.; Vitzthum, V.; Mieville, P.; Alauzun, J.; Roussey, A.; Thieuleux, C.; Mehdi, A.; Bodenhausen, G.; Coperet, C.; Emsley, L. Surface enhanced NMR spectroscopy by dynamic nuclear polarization. *J. Am. Chem. Soc.* **2010**, *132*, 15459−61.

(3) Rosay, M.; Tometich, L.; Pawsey, S.; Bader, R.; Schauwecker, R.; Blank, M.; Borchard, P. M.; Cauffman, S. R.; Felch, K. L.; Weber, R. T.; Temkin, R. J.; Griffin, R. G.; Maas, W. E. Solid-state dynamic nuclear polarization at 263 GHz: spectrometer design and experimental results. *Phys. Chem. Chem. Phys.* **2010**, *12*, 5850−60.

(4) Potapov, A.; Thurber, K. R.; Yau, W. M.; Tycko, R. Dynamic nuclear polarization-enhanced (1)H-(1)(3)C double resonance NMR in static samples below 20 K. *J. Magn. Reson.* **2012**, *221*, 32−40.

(5) Dumez, J. N.; Milani, J.; Vuichoud, B.; Bornet, A.; Lalande-Martin, J.; Tea, I.; Yon, M.; Maucourt, M.; Deborde, C.; Moing, A.; Frydman, L.; Bodenhausen, G.; Jannin, S.; Giraudeau, P. Hyperpolarized NMR of plant and cancer cell extracts at natural abundance. *Analyst* **2015**, *140*, 5860−5863.

(6) Miclet, E.; Abergel, D.; Bornet, A.; Milani, J.; Jannin, S.; Bodenhausen, G. Toward Quantitative Measurements of Enzyme Kinetics by Dissolution Dynamic Nuclear Polarization. *J. Phys. Chem. Lett.* **2014**, *5*, 3290−5.

(7) Wilson, D. M.; Kurhanewicz, J. Hyperpolarized C-13 MR for Molecular Imaging of Prostate Cancer. *J. Nucl. Med.* **2014**, *55*, 1567−1572.

(8) Tayler, M. C.; Marco-Rius, I.; Kettunen, M. I.; Brindle, K. M.; Levitt, M. H.; Pileio, G. Direct enhancement of nuclear singlet order by dynamic nuclear polarization. *J. Am. Chem. Soc.* **2012**, *134*, 7668−71.

(9) Ardenkjaer-Larsen, J. H.; Fridlund, B.; Gram, A.; Hansson, G.; Hansson, L.; Lerche, M. H.; Servin, R.; Thaning, M.; Golman, K. Increase in signal-to-noise ratio of > 10,000 times in liquid-state NMR. *Proc. Natl. Acad. Sci. U. S. A.* **2003**, *100*, 10158−63.

(10) Kurzbach, D.; Canet, E.; Flamm, A. G.; Jhajharia, A.; Weber, E. M.; Konrat, R.; Bodenhausen, G. Investigation of Intrinsically Disordered Proteins through Exchange with Hyperpolarized Water. *Angew. Chem., Int. Ed.* **2017**, *56*, 389−392.

(11) Chappuis, Q.; Milani, J.; Vuichoud, B.; Bornet, A.; Gossert, A. D.; Bodenhausen, G.; Jannin, S. Hyperpolarized Water to Study Protein-Ligand Interactions. *J. Phys. Chem. Lett.* **2015**, *6*, 1674−1678.

(12) Abragam, A.; Goldman, M. Principles of Dynamic Nuclear-Polarization. *Rep. Prog. Phys.* **1978**, *41*, 395−467.

(13) Leavesley, A.; Shimon, D.; Siaw, T. A.; Feintuch, A.; Goldfarb, D.; Vega, S.; Kaminker, I.; Han, S. Effect of electron spectral diffusion on static dynamic nuclear polarization at 7 T. *Phys. Chem. Chem. Phys.* **2017**, *19*, 3596−3605.

(14) Shimon, D.; Hovav, Y.; Feintuch, A.; Goldfarb, D.; Vega, S. Dynamic nuclear polarization in the solid state: a transition between the cross effect and the solid effect. *Phys. Chem. Chem. Phys.* **2012**, *14*, 5729−5743.

(15) Wenckebach, W. T. Dynamic nuclear polarization via thermal mixing: Beyond the high temperature approximation. *J. Magn. Reson.* **2017**, *277*, 68−78.

(16) Hovav, Y.; Feintuch, A.; Vega, S. Theoretical aspects of dynamic nuclear polarization in the solid state - spin temperature and thermal mixing. *Phys. Chem. Chem. Phys.* **2013**, *15*, 188−203.

(17) Serra, S. C.; Rosso, A.; Tedoldi, F. Electron and nuclear spin dynamics in the thermal mixing model of dynamic nuclear polarization. *Phys. Chem. Chem. Phys.* **2012**, *14*, 13299−13308.

(18) Cox, S. F. J.; Bouffard, V.; Goldman, M. The coupling of two nuclear Zeeman reservoirs by the electronic spin-spin reservoir. *J. Phys. C: Solid State Phys.* **1973**, *6*, L100−L103.

(19) Wenckebach, T. *Essentials of Dynamic Nuclear Polarization*; Spindrift Publications: The Netherlands, 2016.

(20) Hovav, Y.; Levinkron, O.; Feintuch, A.; Vega, S. Theoretical Aspects of Dynamic Nuclear Polarization in the Solid State: The Influence of High Radical Concentrations on the Solid Effect and Cross Effect Mechanisms. *Appl. Magn. Reson.* **2012**, *43*, 21−41.

(21) Hovav, Y.; Feintuch, A.; Vega, S. Theoretical aspects of dynamic nuclear polarization in the solid state - The cross effect. *J. Magn. Reson.* **2012**, *214*, 29−41.

(22) Hovav, Y.; Feintuch, A.; Vega, S. Theoretical aspects of dynamic nuclear polarization in the solid state - The solid effect. *J. Magn. Reson.* **2010**, *207*, 176−189.

(23) Sauvee, C.; Casano, G.; Abel, S.; Rockenbauer, A.; Akhmetzyanov, D.; Karoui, H.; Siri, D.; Aussenac, F.; Maas, W.; Weber, R. T.; Prisner, T.; Rosay, M.; Tordo, P.; Ouari, O. Tailoring of Polarizing Agents in the bTurea Series for Cross-Effect Dynamic Nuclear Polarization in Aqueous Media. *Chem. - Eur. J.* **2016**, *22*, 5598−606.

(24) Weber, E. M. M.; Vezin, H.; Kempf, J. G.; Bodenhausen, G.; Abergel, D.; Kurzbach, D. Anisotropic longitudinal electronic relaxation affects DNP at cryogenic temperatures. *Phys. Chem. Chem. Phys.* **2017**, *19*, 16087−16094.

(25) Kurzbach, D.; Weber, E. M. M.; Jhajharia, A.; Cousin, S. F.; Sadet, A.; Marhabaie, S.; Canet, E.; Birlirakis, N.; Milani, J.; Jannin, S.; Eshchenko, D.; Hassan, A.; Melzi, R.; Luetolf, S.; Sacher, M.; Rossire, M.; Kempf, J.; Lohman, J. A. B.; Weller, M.; Bodenhausen, G.; Abergel, D. Dissolution Dynamic Nuclear Polarization of Deuterated Molecules Enhanced by Cross-Polarization. *J. Chem. Phys.* **2016**, *145*, 194203.

(26) Jannin, S.; Bornet, A.; Colombo, S.; Bodenhausen, G. Low-temperature cross polarization in view of enhancing dissolution Dynamic Nuclear Polarization in NMR. *Chem. Phys. Lett.* **2011**, *517*, 234−236.

(27) De Luca, A.; Rosso, A. Dynamic nuclear polarization and the paradox of Quantum Thermalization. *Phys. Rev. Lett.* **2015**, *115*, 080401-1−080401-5.

(28) De Luca, A.; Rodriguez-Arias, I.; Mueller, M.; Rosso, A. Thermalization and many-body localization in systems under dynamic nuclear polarization. *Phys. Rev. B: Condens. Matter Mater. Phys.* **2016**, *94*, 014203-1−014203-15.

(29) Siaw, T. A.; Fehr, M.; Lund, A.; Latimer, A.; Walker, S. A.; Edwards, D. T.; Han, S. I. Effect of electron spin dynamics on solid-state dynamic nuclear polarization performance. *Phys. Chem. Chem. Phys.* **2014**, *16*, 18694−18706.

(30) Serra, S. C.; Rosso, A.; Tedoldi, F. On the role of electron-nucleus contact and microwave saturation in thermal mixing DNP. *Phys. Chem. Chem. Phys.* **2013**, *15*, 8416−8428.